ARMY RESEARCH LABORATORY

Characterization and Consolidation of Tungsten Nanopowders Produced by Salt-Assisted Combustion Synthesis

by Bradley R. Klotz, Franklyn R. Kellogg, and Kyu C. Cho

ARL-TR-5311 **September 2010**

NOTICES

Disclaimers

The findings in this report are not to be construed as an official Department of the Army position unless so designated by other authorized documents.

Citation of manufacturer's or trade names does not constitute an official endorsement or approval of the use thereof.

Destroy this report when it is no longer needed. Do not return it to the originator.

Army Research Laboratory
Aberdeen Proving Ground, MD 21005-5069

ARL-TR-5311 **September 2010**

Characterization and Consolidation of Tungsten Nanopowders Produced by Salt-Assisted Combustion Synthesis

Bradley R. Klotz
Dynamic Science, Inc.

Franklyn R. Kellogg
Data Matrix Solutions

Kyu C. Cho
Weapons and Materials Research Directorate, ARL

REPORT DOCUMENTATION PAGE	Form Approved OMB No. 0704-0188

1. REPORT DATE *(DD-MM-YYYY)*	2. REPORT TYPE	3. DATES COVERED (From - To)
September 2010	Final	November 2006–July 2007

4. TITLE AND SUBTITLE
Characterization and Consolidation of Tungsten Nanopowders Produced by Salt-Assisted Combustion Synthesis

5a. CONTRACT NUMBER

5b. GRANT NUMBER

5c. PROGRAM ELEMENT NUMBER

6. AUTHOR(S)
Bradley R. Klotz,[*] Franklyn R. Kellogg[†], and Kyu C. Cho

5d. PROJECT NUMBER
1L162618AH8

5e. TASK NUMBER

5f. WORK UNIT NUMBER

7. PERFORMING ORGANIZATION NAME(S) AND ADDRESS(ES)
U.S. Army Research Laboratory
ATTN: RDRL-WMM-F
Aberdeen Proving Ground, MD 21005

8. PERFORMING ORGANIZATION REPORT NUMBER
ARL-TR-5311

9. SPONSORING/MONITORING AGENCY NAME(S) AND ADDRESS(ES)

10. SPONSOR/MONITOR'S ACRONYM(S)

11. SPONSOR/MONITOR'S REPORT NUMBER(S)

12. DISTRIBUTION/AVAILABILITY STATEMENT
Approved for public release; distribution is unlimited.

13. SUPPLEMENTARY NOTES
[*]Dynamic Science, Inc., Aberdeen Proving Ground, MD 21005-5069
[†]Data Matrix Solutions, Aberdeen Proving Ground, MD 21005-5069

14. ABSTRACT
Tungsten nanopowders have been produced at Chungnam National University in Daejeon, South Korea, by a salt-assisted combustion synthesis method. Samples of these powders were obtained and characterized to determine particle size, morphology, degree of agglomeration, and chemical purity. The powders were shown to consist of nano-sized particles agglomerated into larger clusters and were found to contain higher levels of oxygen than conventional fine tungsten powder. The powders were then consolidated by the Plasma Pressure Compaction (P^2C) method. The resulting samples were examined to determine density, grain size, and chemical purity. Although bulk samples were produced containing nano-sized grains, high density was not achieved. However, when compared with samples consolidated using conventional sub-micron tungsten powder, higher density was achieved at the lower processing temperatures required for retention of initial grain size.

15. SUBJECT TERMS
tungsten, nanopowder, plasma pressure compaction

16. SECURITY CLASSIFICATION OF:			17. LIMITATION OF ABSTRACT	18. NUMBER OF PAGES	19a. NAME OF RESPONSIBLE PERSON
a. REPORT	b. ABSTRACT	c. THIS PAGE			Bradley R. Klotz
Unclassified	Unclassified	Unclassified	UU	32	19b. TELEPHONE NUMBER (*Include area code*) 410-306-2130

Standard Form 298 (Rev. 8/98)
Prescribed by ANSI Std. Z39.18

Contents

List of Figures

List of Tables

INTENTIONALLY LEFT BLANK.

1. Introduction

1.1 Objective

Researchers at Chungnam National University (CNU) in Daejeon, South Korea have used a salt-assisted combustion synthesis method to synthesize tungsten nanopowders using a mixture of tungsten trioxide, zinc, and sodium chloride (WO_3+Zn+NaCl). The following report details efforts to evaluate these tungsten powders for use in the consolidation of bulk nanocrystalline samples. Particle size, morphology, degree of agglomeration, and chemical purity of the starting powder were examined using a variety of powder characterization techniques. Consolidation of the powders was carried out by Plasma Pressure Compaction (P^2C). Resulting samples were examined to evaluate properties such as density, grain size, and chemical purity. Results were compared with those achieved for submicron-sized tungsten powder.

1.2 Background

Because of its high density, tungsten has been considered as a candidate material to replace depleted uranium (DU) in kinetic-energy penetrators. DU is currently used due to its high density, as well as its tendency to form adiabatic shear bands as the penetrator enters a target, resulting in a chiseled nose and increased penetration depth (*1*). It is tungsten's resistance to this adiabatic shear localization that limits its applicability in anti-armor applications (*2*). Studies of nanocrystalline (<100 nm) and ultra-fine grain (UFG) (<300 nm) iron have shown that reducing the grain size of the material results in a tendency for deformation during quasi-static testing to occur by shear banding as opposed to the uniform deformation seen in conventional grain-sized iron (*3*). Moreover, recent studies have shown that when tungsten grains are refined to the nanocrystalline and ultra-fine grain (UFG) regime by severe plastic deformation techniques, reduced strain rate sensitivity and localized shearing are observed (*4*, *5*). Thus, a penetrator made of nanocrystalline tungsten could possibly duplicate the performance of DU.

The consolidation of nano-sized tungsten powder by a technique that will result in the retention of initial grain size is one method of producing bulk nanocrystalline parts. Properties of the starting powder, such as chemical purity, particle size, size distribution, morphology, and degree of agglomeration are important factors that determine the densification behavior of a powder. Thus, powder characterization is an important step prior to consolidation. Experiments have already been undertaken at the U.S. Army Research Laboratory (ARL) to consolidate fine-grained and nano-sized tungsten by the Plasma Pressure Compaction (P^2C) method (*6*, *7*). The P^2C method subjects powder in a graphite die to high current DC voltage, enabling rapid heating rates and very short high-temperature hold times. Submicron tungsten powder has been previously consolidated by P^2C to ~97% theoretical density (*7*). However, the high density of the consolidated samples came at the expense of grain growth, with final grain sizes approximately

10 times the initial particle size. The use of nanocrystalline tungsten powders could provide for a sample with final grain size in the nanocrystalline regime. The study detailed in this report seeks to compare the powder characteristics and consolidation behavior of the CNU-produced nanocrystalline tungsten powders mentioned previously to those of conventional submicron tungsten powder.

2. Experimental Procedure

Four different grades of CNU-synthesized tungsten powder were selected for analysis and consolidation. The CNU powders were designated tungsten powder nos. 1, 2, 3, and 14. Powder data provided by CNU for each of the powders is shown in table 1. Powder nos. 1 and 2 were different lots of particles synthesized by the same method. Powder no. 3 was produced under slightly different conditions than the first two powders. Powder no. 14 was similar to powder no. 1, but a secondary heat treatment was performed by CNU to reduce oxygen concentration in the final powder. Powder characteristics and consolidation data obtained previously for Osram Sylvania M10-grade tungsten powder (manufacturer specified particle size: 0.60–0.90 μm) and Teledyne Wah Chang tungsten powder (manufacturer specified particle size: 0.70–0.99 μm) were used for comparison with the nanopowders (*6*, *7*). The size and morphology of the as-received nanopowders were observed on a Hitachi S-4700 field emission scanning electron microscope (FESEM) with energy dispersive x-ray spectroscopy (EDS) capabilities. Samples of each powder were also dispersed in a water-glycerol mixture, and the particle size distribution (PSD) was determined by laser scattering techniques on a Horiba LA-910 Laser Scattering Particle Size Distribution Analyzer. Elemental chemical analysis of the powders was carried out by Luvak, Inc. of Boylston, MA. The amount of sulfur and carbon was determined by combustion infrared detection, oxygen content was measured by inert gas fusion, and all other elements were measured by direct current plasma emission spectroscopy. Powder nos. 1, 2, and 3 were initially sent out for measurement of only carbon and oxygen content. A sample of powder no. 14 and an additional sample of powder no. 1 were also sent for measurement of a broader spectrum of elements to examine the difference that hydrogen heat treatment made in impurity content. In addition, an x-ray diffraction (XRD) pattern to detect the presence of impurity phases was generated for each powder on a Phillips x-ray diffractometer with Phillips X-Pert Analysis software.

Table 1. Powder data from CNU.

Powder	Oxygen Content (weight-percent)	Particle Size (nm)	Quantity (kg)
Tungsten no. 1	1.7	80–90	2.0
Tungsten no. 2	1.7	100–110	0.25
Tungsten no. 3	1.7	200	0.25
Tungsten no. 14	0.25–0.3	80–120	1.4

For the powders obtained from CNU, no treatment was performed at ARL prior to P^2C consolidation. Each powder sample was consolidated in the as-received condition. The development of P^2C processing parameters for tungsten has been described previously (*6*, *7*). For this study, 50 g of the CNU tungsten powders were packed into 1-in-diameter graphite dies and placed between two water cooled platens in the chamber of the P^2C apparatus (figure 1). Samples were loaded at a pressure of 27 MPa. Prior to consolidation, the chamber was pumped down to 10 mTorr or less. All consolidation runs were carried out under vacuum. The samples were first subjected to a pulsed current with 10 µs on/off times. Pulsing currents of 200, 400, 600, 800, and 1000 A were applied in a step-wise fashion, with 5-min intervals at each pulsing step. The temperature of the sample was monitored at the outside surface of the die with an optical pyrometer, although the temperature inside the die is known to be much higher (*8*). The lowest temperature that the pyrometer was capable of reading was 636 °C. The pulsing parameters were run until the pyrometer began to register a temperature reading. For most samples, this occurred after being at 1000 A for 5 min. Once the pyrometer became active, the pressure was increased to 100 MPa, the power supply was switched to constant current mode, and the current was rapidly increased to 5000 A. The applied current of 5000 A was maintained until the sintering temperature was reached, at which point, the current was rapidly lowered to 0 and the sample was allowed to cool under vacuum.

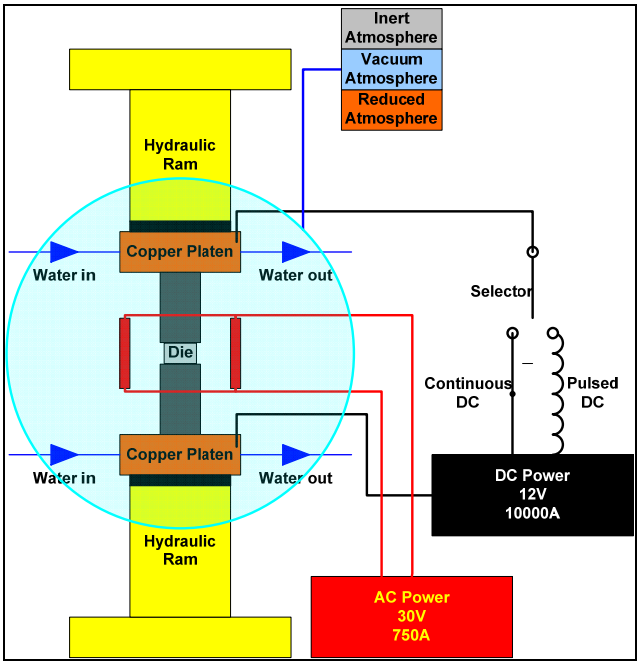

Figure 1. Schematic of the P^2C apparatus.

Once removed from the P^2C chamber, samples were ejected from the die and ground to remove graphite or tungsten carbide on the surface. Density was measured by the Archimedes' method. Samples were then sectioned to provide samples for scanning electron microscopy and x-ray diffraction.

3. Results and Discussion

3.1 Powder Characterization

FESEM micrographs of the four different grades of CNU tungsten nanopowders are shown in figures 2–5. Powder nos. 1 and 2 appeared similar, consisting of fine particles clustered in large agglomerates, some on the order of 10–20 μm. The fine particles in these two powders looked to be less than 100 nm on average, and there appeared to be very little joining between the particles. The sample of powder no. 3 contained less large agglomerates, and the size of the fine particles appeared on the order of those seen in powder nos. 1 and 2. However, their appeared to be more joining between the fine particles in powder no. 3 than in the first two powders. Powder no. 14, which was the same grade as powder no. 1 but had been heat treated by CNU in hydrogen prior to sending to ARL, contained more large agglomerates than the other three powders, the largest being on the order of 50 μm. There also appeared to be some sintering and coalescence of the fine particles as shown in the high magnification images, most likely as a result of the secondary heating cycle. For comparison purposes, FESEM micrographs of the Osram Sylvania M-10 powder are shown in figure 6.

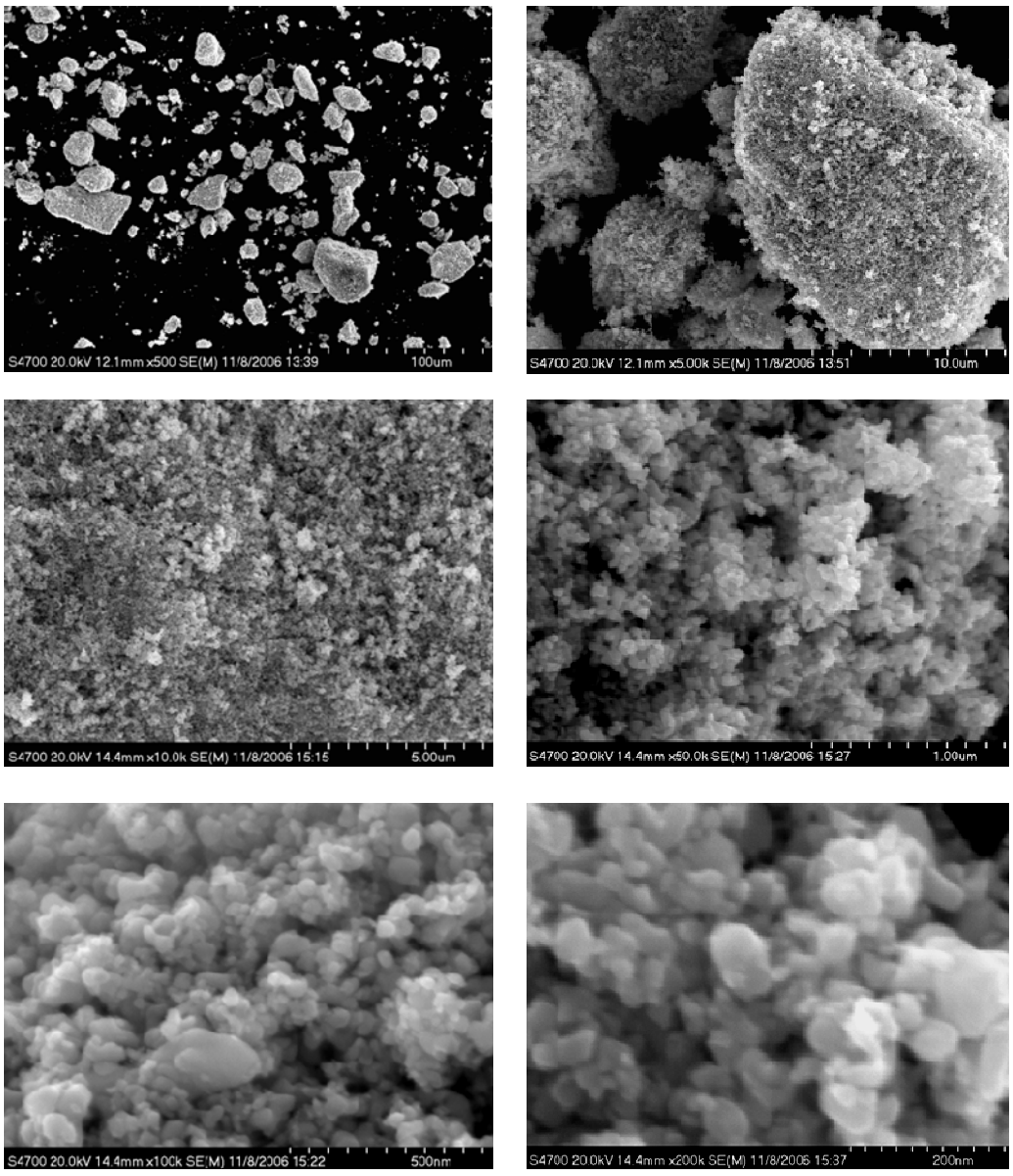

Figure 2. FESEM micrographs of CNU tungsten powder no. 1.

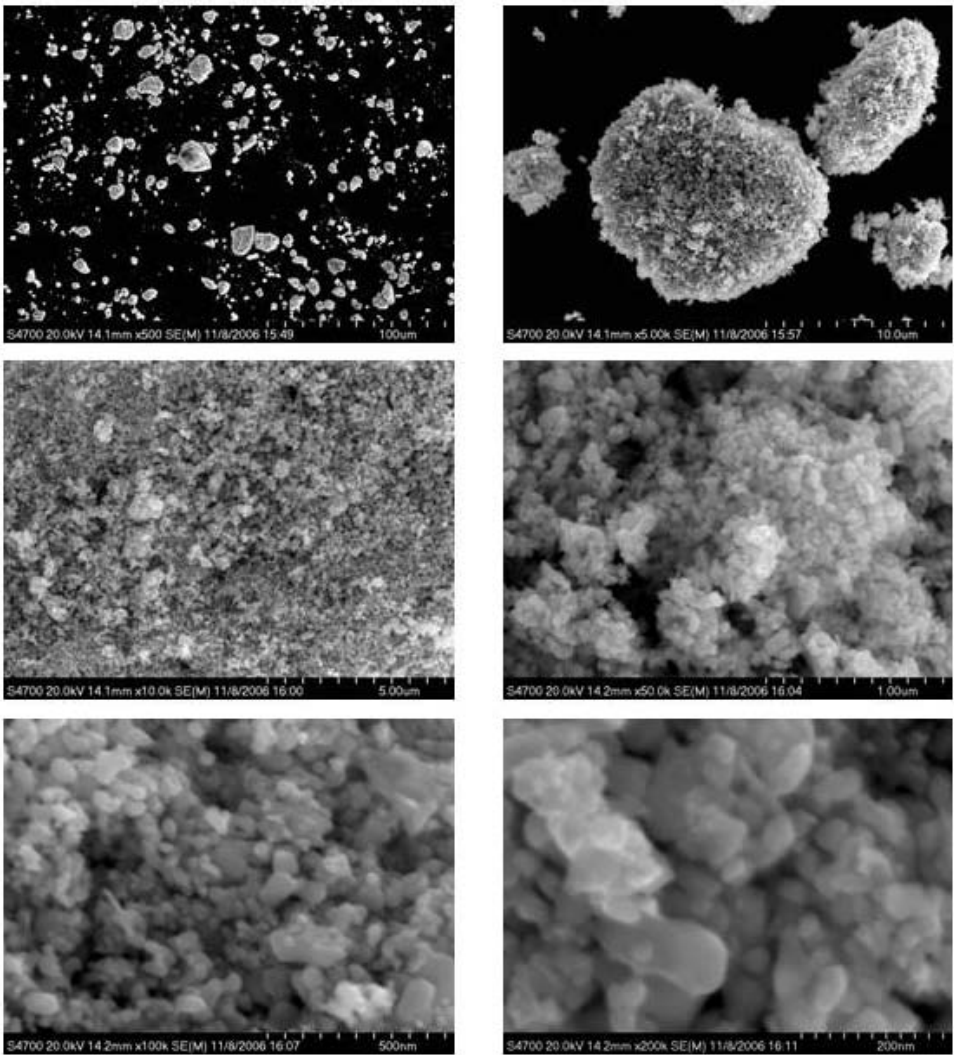

Figure 3. FESEM micrographs of CNU tungsten powder no. 2.

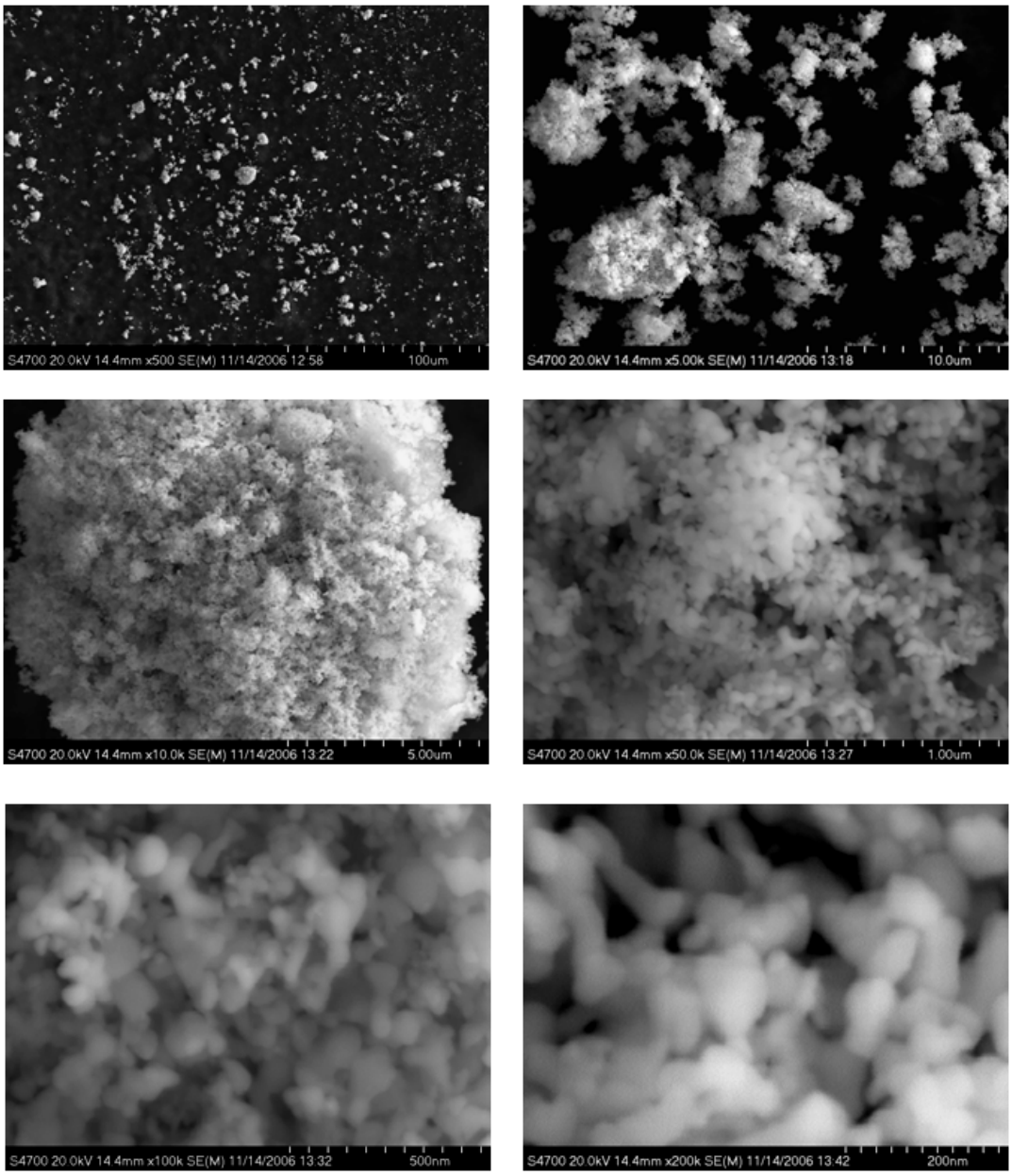

Figure 4. FESEM micrographs of CNU tungsten powder no. 3.

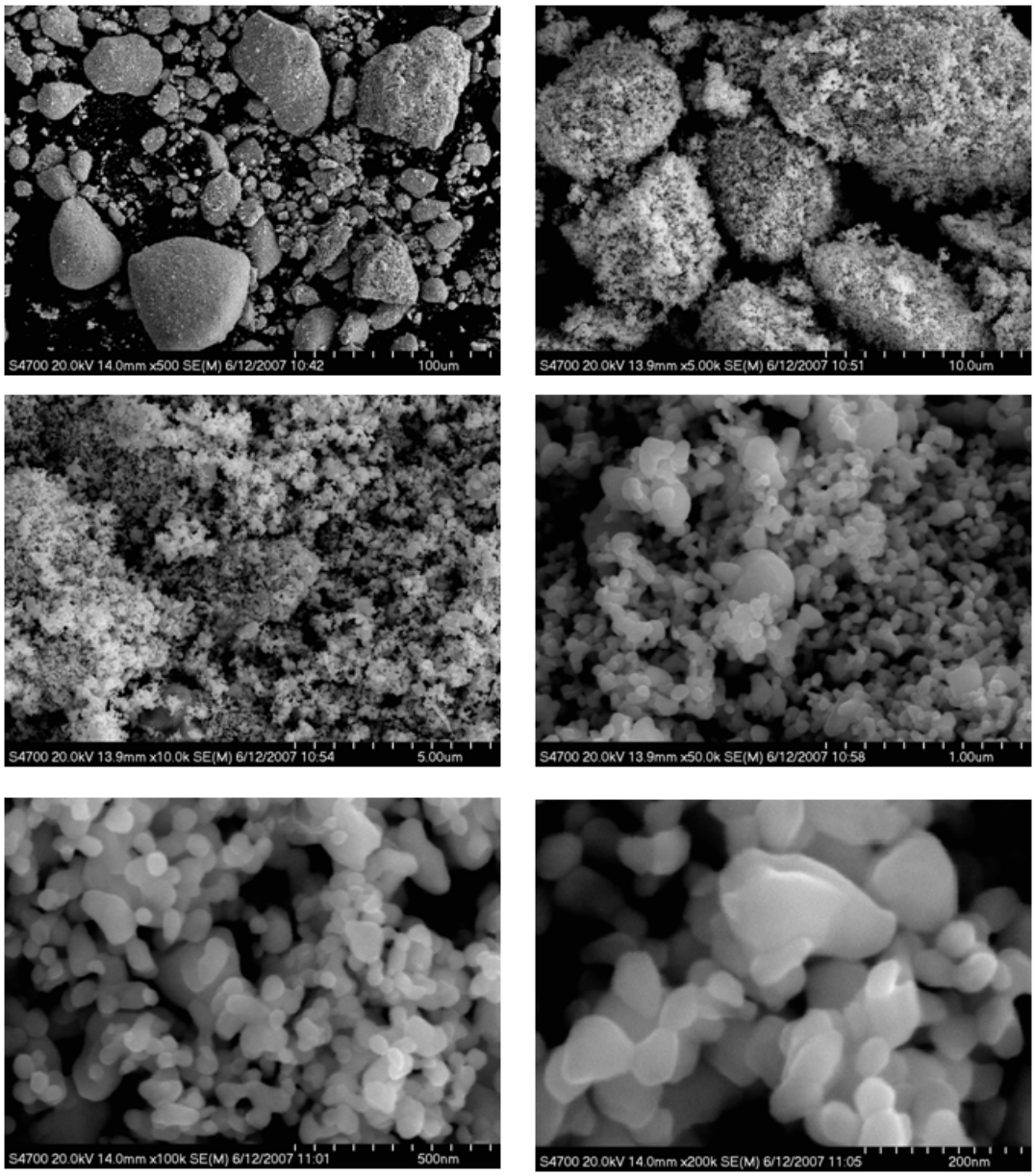

Figure 5. FESEM micrographs of CNU tungsten powder no. 14.

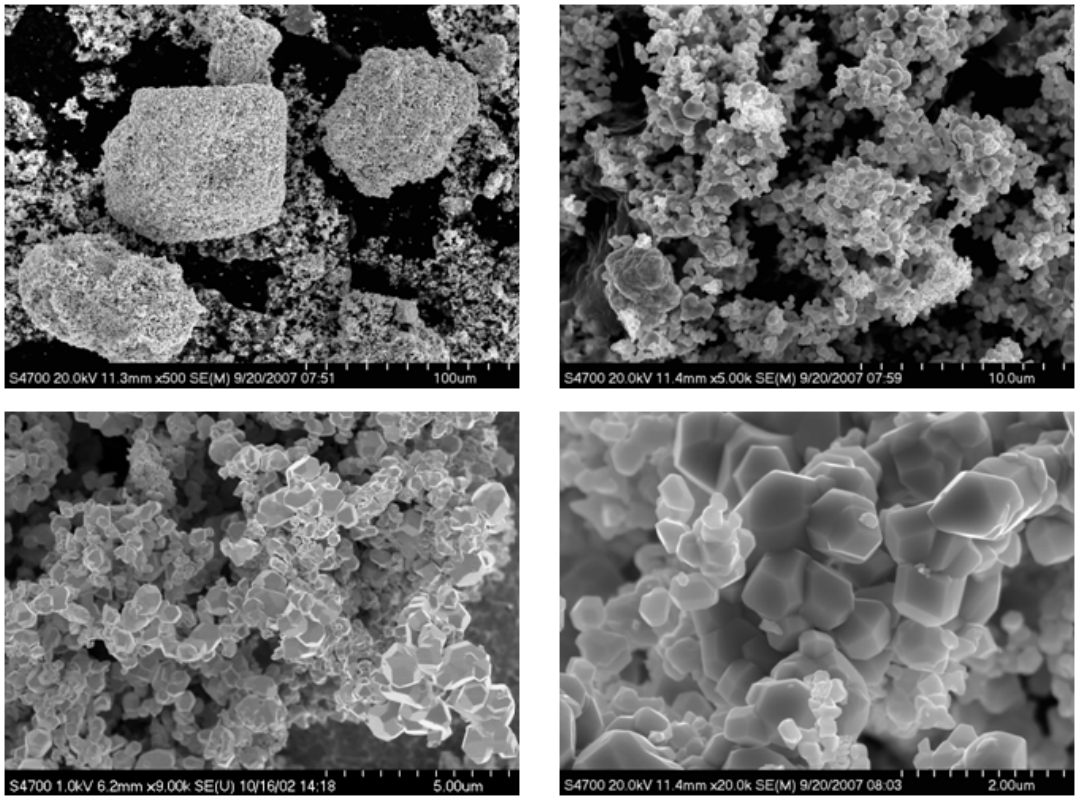

Figure 6. FESEM images of Osram Sylvania M-10 tungsten powder.

Particle size distribution plots, as generated on the Horiba LA-910 for each of the four CNU tungsten powders, are shown in figure 7. The LA-910 is able to detect a wide range of particle sizes, so it is able to distinguish the large agglomerates observed by FESEM. Particle sizes down to <100 nm can be seen in plots for powder nos. 1, 2, and 14. Powder nos. 3 and 14 appeared to show less fine particles, likely due to the joining between the particles seen in the FESEM micrographs.

The results of chemical analysis of CNU powder nos. 1, 2, and 3 for measurement of carbon and oxygen are shown in table 2. The three powders showed consistent levels of both elements in each powder, with the oxygen level being higher than that measured by CNU. Elemental analysis for powder nos. 1 and 14 are shown in table 3. Powder no. 14, which underwent secondary heat treatment in hydrogen after synthesis, contained much less oxygen than powder no. 1, as well as lower levels of carbon and zinc. The Osram Sylvania M-10 tungsten powder was measured to contain 0.59 weight-percent oxygen, which is significantly lower than all but the hydrogen-reduced CNU powder no. 14.

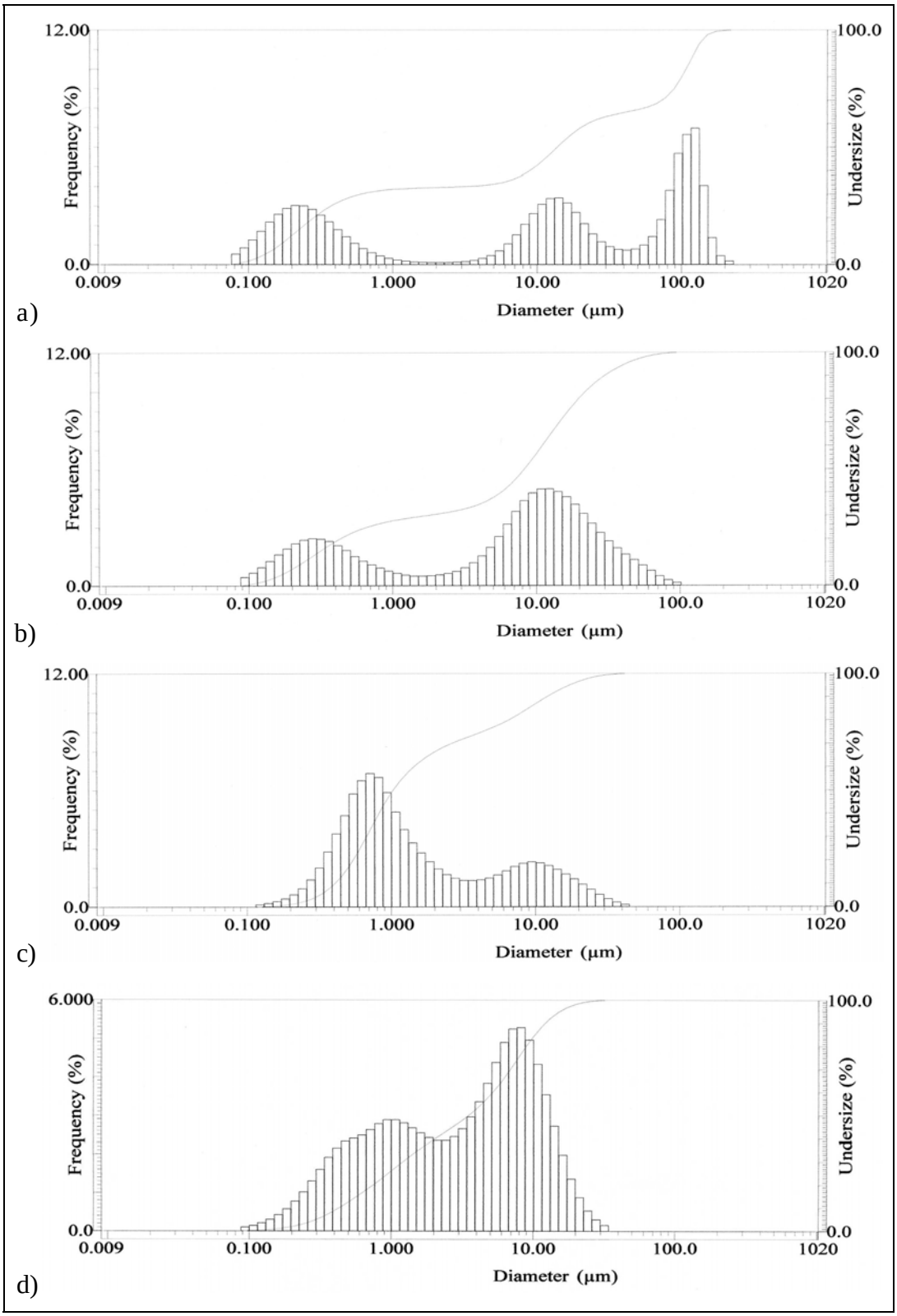

Figure 7. Particle size distribution plots for (a) CNU powder no. 1, (b) CNU powder no. 2, (c) CNU powder no. 3, and (d) CNU powder no. 14.

Table 2. Carbon and oxygen analysis of CNU tungsten powder nos. 1, 2, and 3.

Element	Powder No. 1 (weight-percent)	Powder No. 2 (weight-percent)	Powder No. 3 (weight-percent)
Carbon	0.60	0.46	0.65
Oxygen	2.42	2.38	2.34

Table 3. Elemental analysis of CNU tungsten powder nos. 1 and 14.

Element	Tungsten Powder No. 1 (weight-percent)	Tungsten Powder No. 14 (weight-percent)
Ag	0.0005	0.0005
Al	0.0005	0.0024
As	0.0020	0.0020
Bi	0.0020	0.0020
C	0.0670	0.0250
Ca	0.0005	0.0006
Co	0.0005	0.0005
Cr	0.0005	0.0005
Cu	0.0037	0.0011
Fe	0.0005	0.0010
Mg	0.0005	0.0005
Mo	0.0005	0.0005
N	0.6600	0.0380
Ni	0.0005	0.0005
O	2.8000	0.3500
P	0.0020	0.0020
Pb	0.0780	0.0010
S	0.0030	0.0020
Sb	0.0020	0.0020
Si	0.0030	0.0030
Sn	0.0020	0.0020
Ti	0.0005	0.0005
V	0.0005	0.0005
Zn	1.3100	0.5200
Zr	0.0650	0.0170

X-ray diffraction patterns for the four CNU tungsten powders are shown in figure 8. Powder nos. 1 and 2 appeared similar, with no significant peaks for phases other than tungsten visible. Powder no. 3 was seen to contain peaks for tungsten oxide. Powder no. 14, which had the lowest oxygen content as determined by chemical analysis, also did not show a significant amount of any phases other than tungsten.

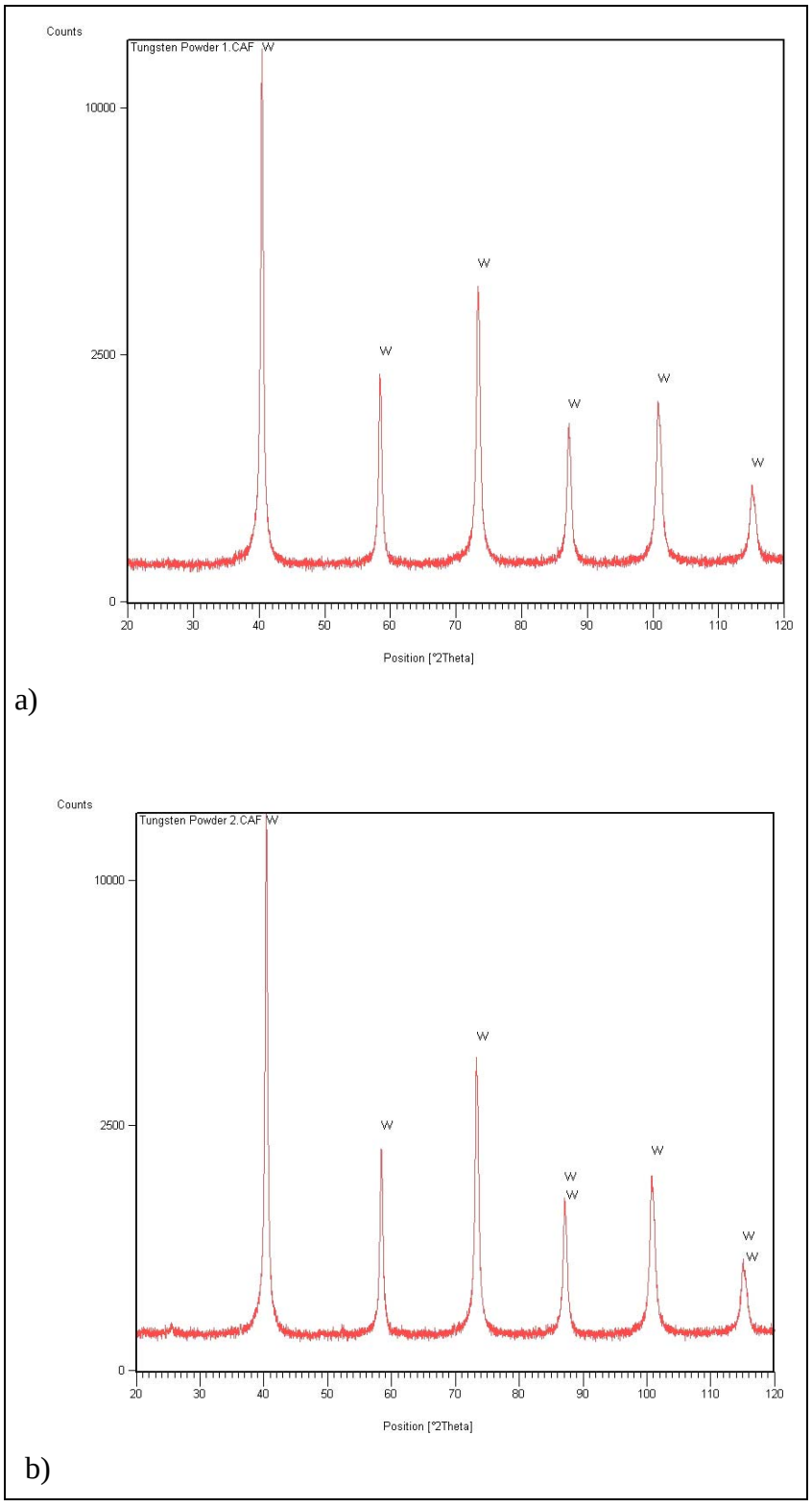

Figure 8. X-ray diffraction patterns for (a) CNU tungsten powder no. 1, (b) CNU tungsten powder no. 2, (c) CNU tungsten powder no. 3, and (d) CNU tungsten powder no. 14.

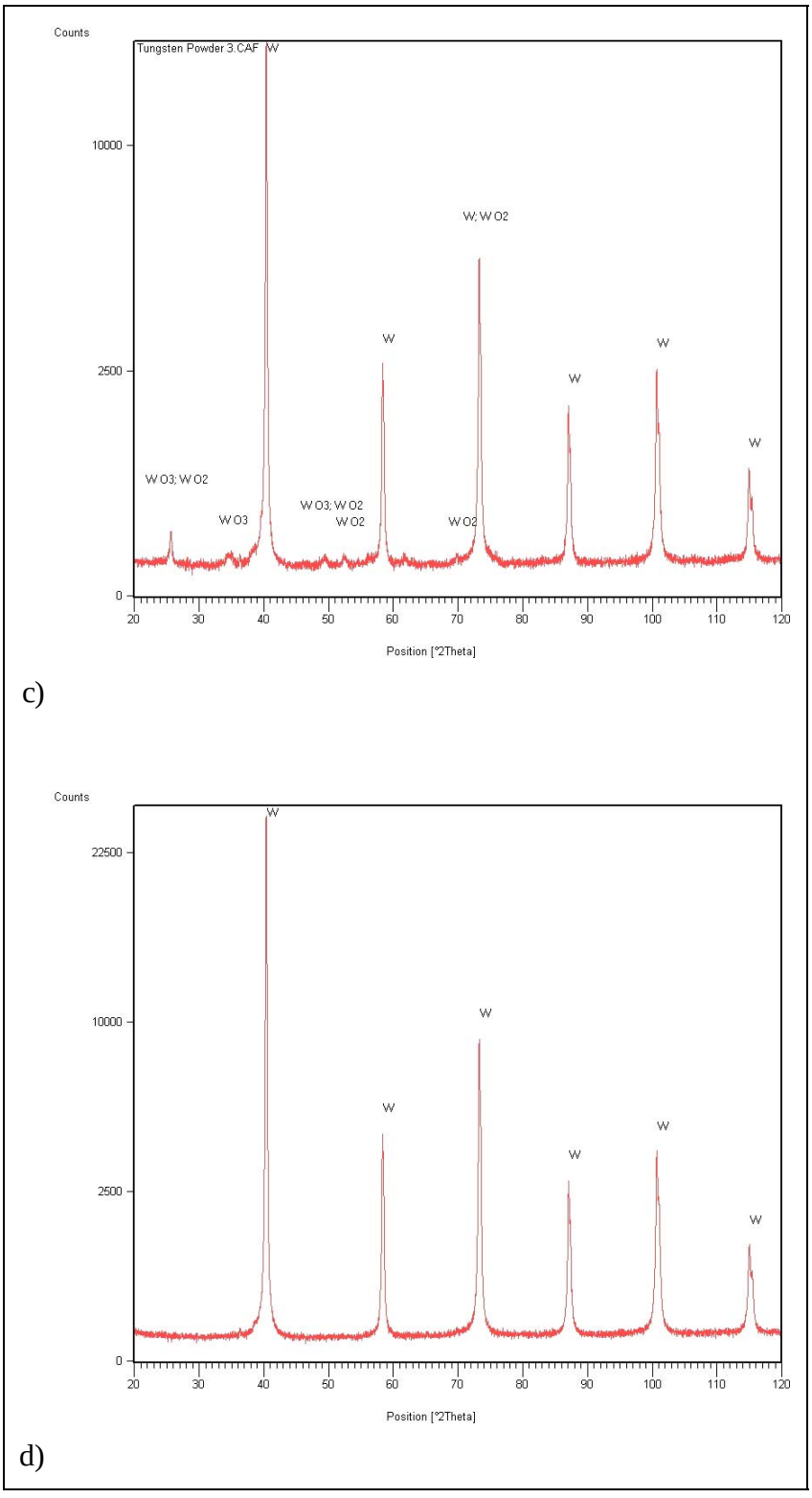

Figure 8. X-ray diffraction patterns for (a) CNU tungsten powder no. 1, (b) CNU tungsten powder no. 2, (c) CNU tungsten powder no. 3, and (d) CNU tungsten powder no. 14 (continued).

3.2 Powder Consolidation

Based on the results of a previous study on consolidation of nano-scale tungsten powder (*9*), it was decided that a lower temperature would be used for P^2C consolidation of the four CNU tungsten powders in an attempt to retain initial grain size. Thus, all four CNU samples were consolidated with a final consolidation temperature of 1200 °C. No pre-treatment of the powders was done prior to consolidation. Densities of the four samples are shown in table 4. FESEM photos are shown in figures 9–12.

Table 4. Densities of CNU tungsten P^2C samples.

Powder No.	Consolidation Temperature (ºC)	Density (g/cm^3)	Theoretical Density (°)
1	1200	14.73	76.3
2	1200	15.27	79.1
3	1200	15.57	80.7
14	1200	15.06	78.0

None of the consolidated samples of CNU powder were able to achieve full density at the temperature used. Despite the sample made with powder no. 2 having a slightly higher density when compared with the sample made with powder no. 1, the samples had similar microstructures as seen in the FESEM images in figures 9 and 10. The structure appeared irregular, with areas of higher density and areas containing porosity and oxide phases. The grain size for these two samples was similar. The sample made with powder no. 3 as shown in figure 11 had a more uniform microstructure and a finer grain size than the previous two specimens, but also contained a large amount of porosity and oxide phases. The consolidated sample of powder no. 14 (figure 12) showed little or no oxide phases and had an irregular microstructure containing well-sintered areas and areas of porosity. The grain size of this sample was similar to that of the powder no. 3 sample. Figure 13 shows the XRD patterns for each of the consolidated samples. The samples from powder nos. 1, 2, and 3 now exhibit tungsten oxide (WO_2) peaks, which were only evident prior to consolidation in powder no. 3. This oxide phase, which could be seen in the FESEM images, must have formed during consolidation due to the high oxygen content of the powders. The powder no. 14 sample, which used powder that underwent hydrogen reduction heat treatment to reduce the oxygen level, showed no significant oxide peaks.

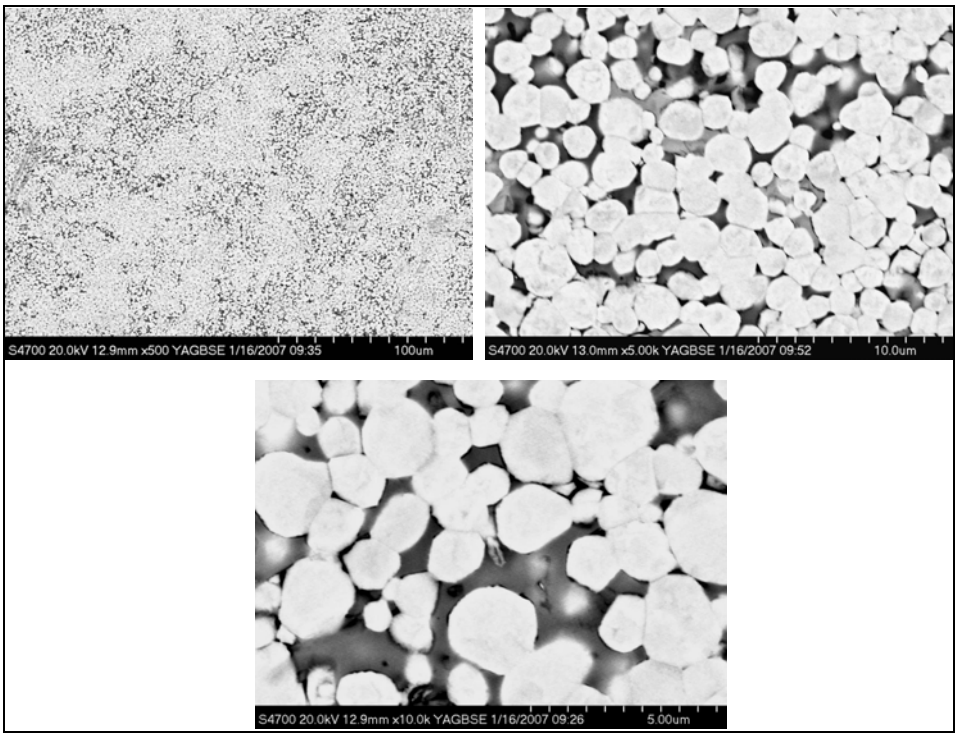

Figure 9. FESEM micrographs of consolidated CNU tungsten powder no. 1.

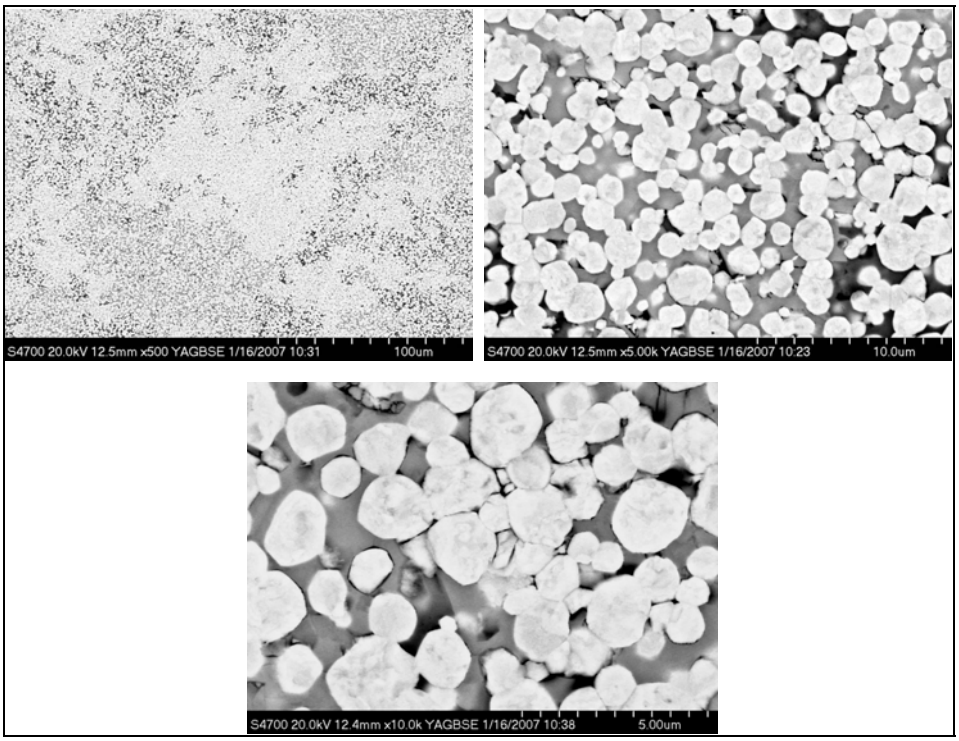

Figure 10. FESEM micrographs of consolidated CNU tungsten powder no. 2.

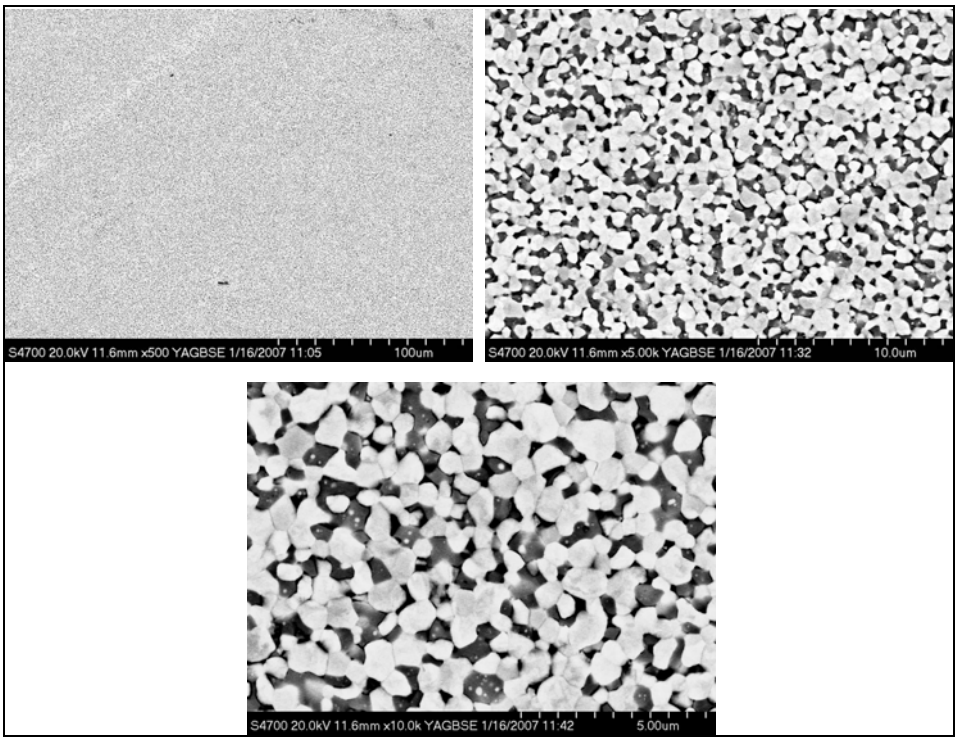

Figure 11. FESEM micrographs of consolidated CNU tungsten powder no. 3.

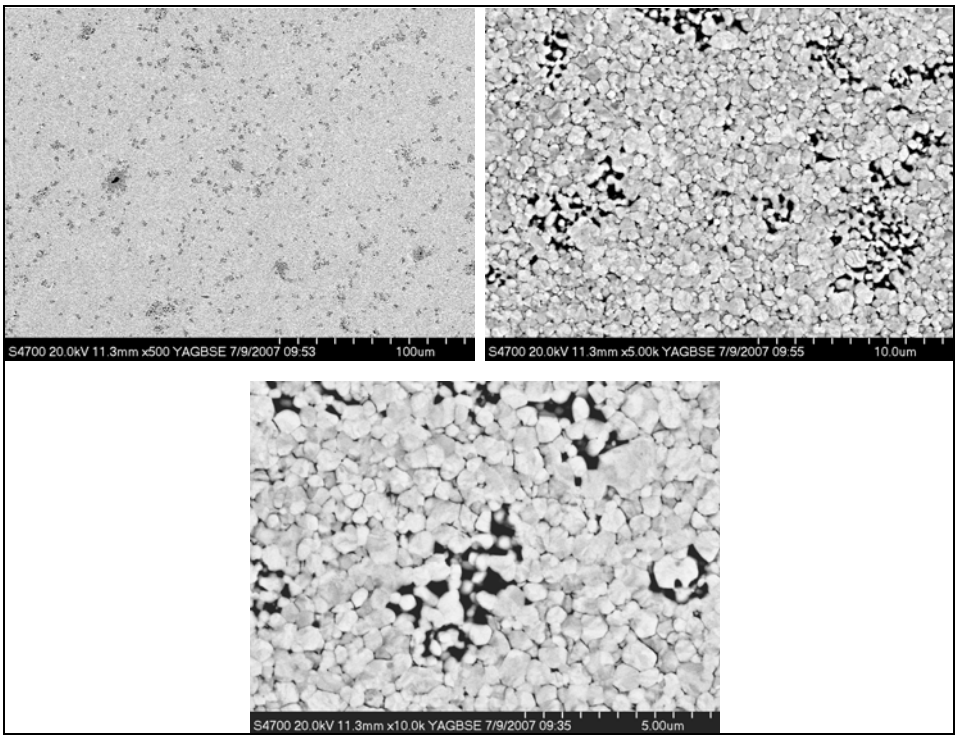

Figure 12. FESEM micrographs of consolidated CNU tungsten powder no. 14.

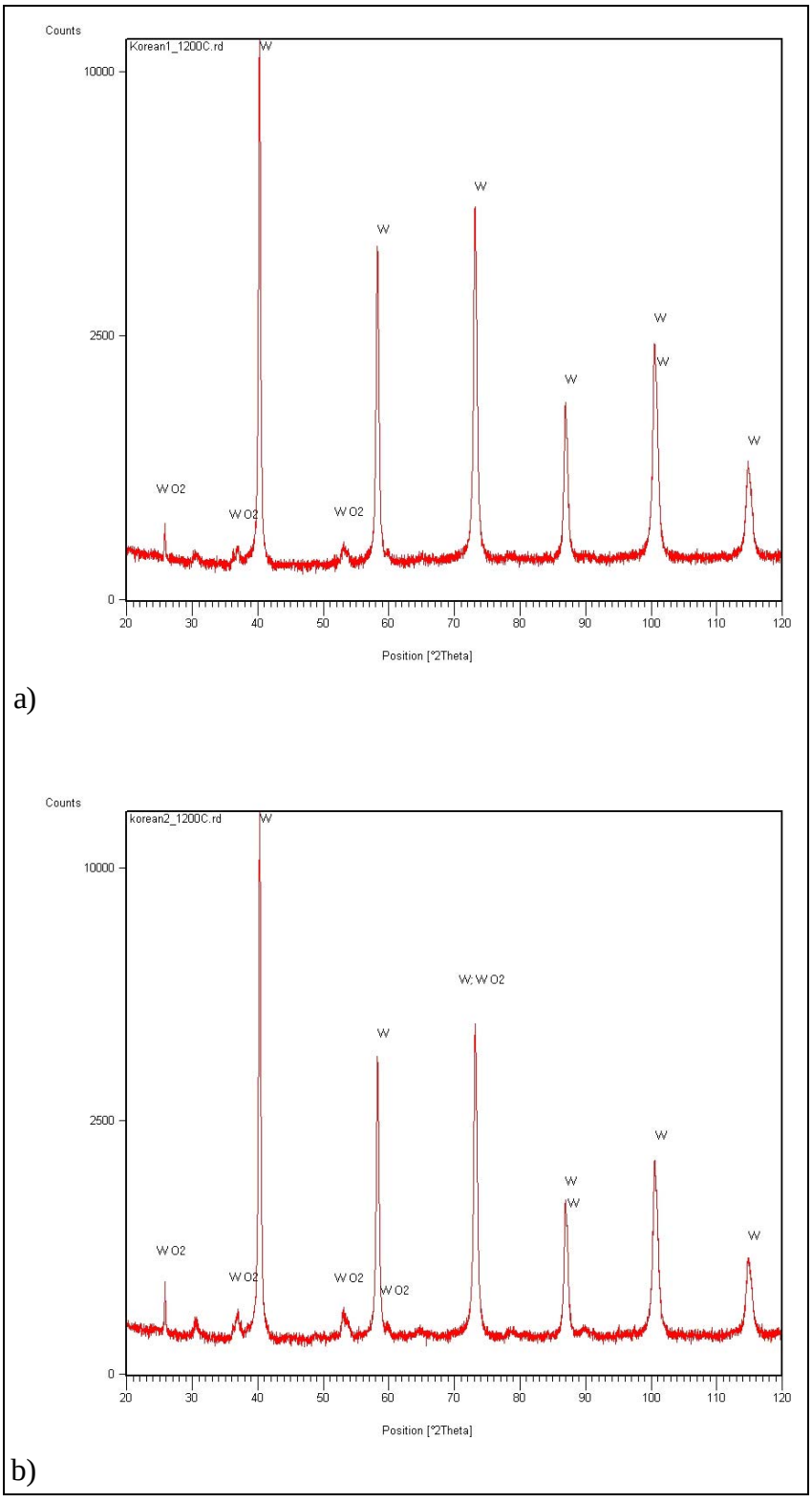

Figure 13. X-ray diffraction patterns for consolidated samples of (a) powder no. 1, (b) powder no. 2, (c) powder no. 3, and (d) powder no. 14.

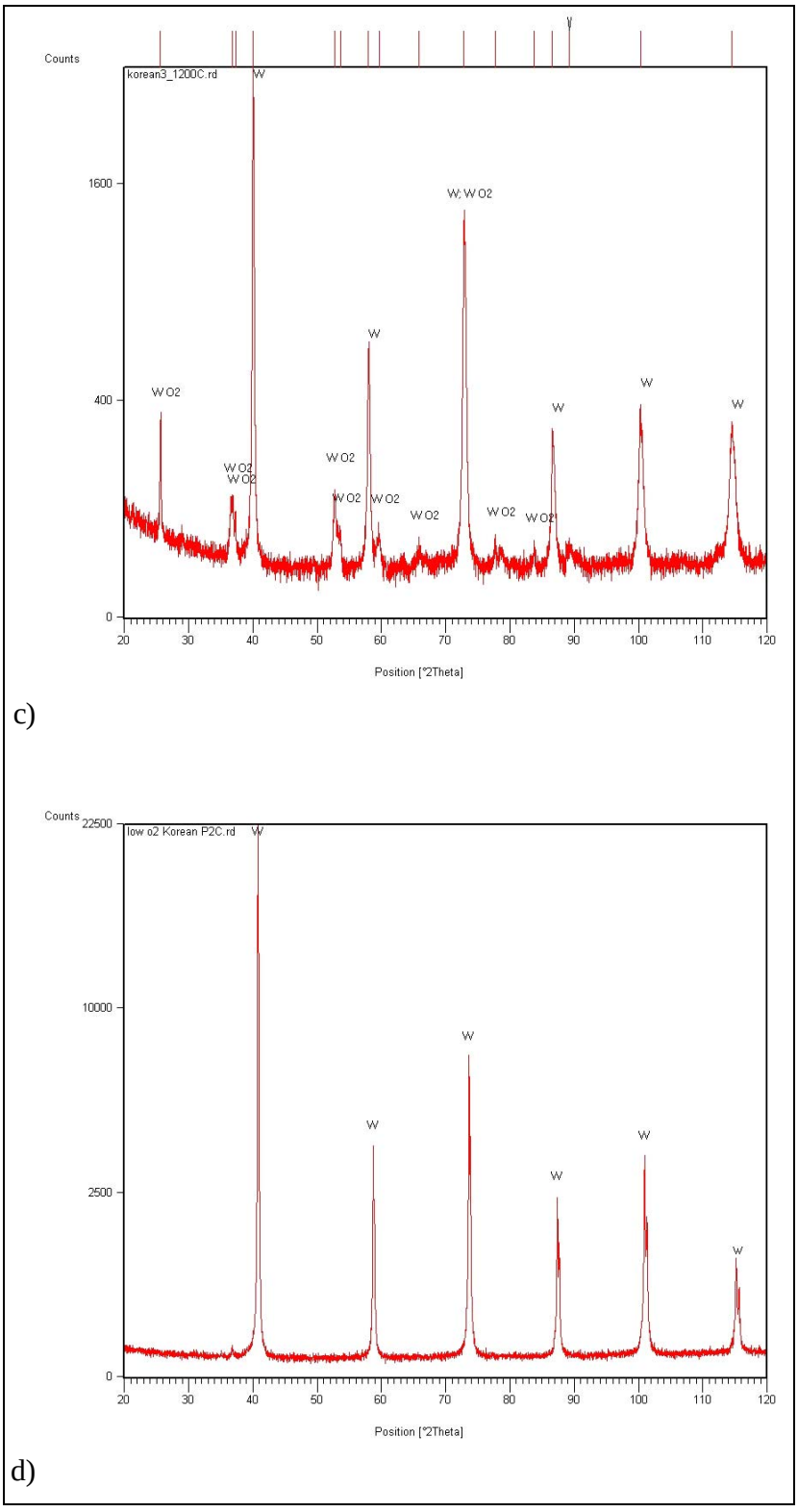

Figure 13. X-ray diffraction patterns for consolidated samples of (a) powder no. 1, (b) powder no. 2, (c) powder no. 3, and (d) powder no. 14 (continued).

A previous study produced specimens of Osram Sylvania M-10 tungsten powder consolidated by P^2C at a temperature of 1700 ºC and a pressure of 65 MPa using different powder treatments prior to consolidation (*7*). Powder pretreatment processes included hydrogen heat treatment of the powder in a graphite die before loading into the P^2C chamber, and the application of pulsed current before the final consolidation step. Densities for the M-10 consolidated samples are shown in table 5. FESEM micrographs can be seen in figure 14.

Table 5. Densities of Osram Sylvania M-10 tungsten P^2C samples.

Powder Pretreatment	**Density (g/cm^3)**	**Theoretical Density (°)**
None	17.49	90.6
Hydrogen reduction	18.28	94.7
Pulsing	18.39	95.3
Hydrogen reduction and pulsing	18.70	96.9

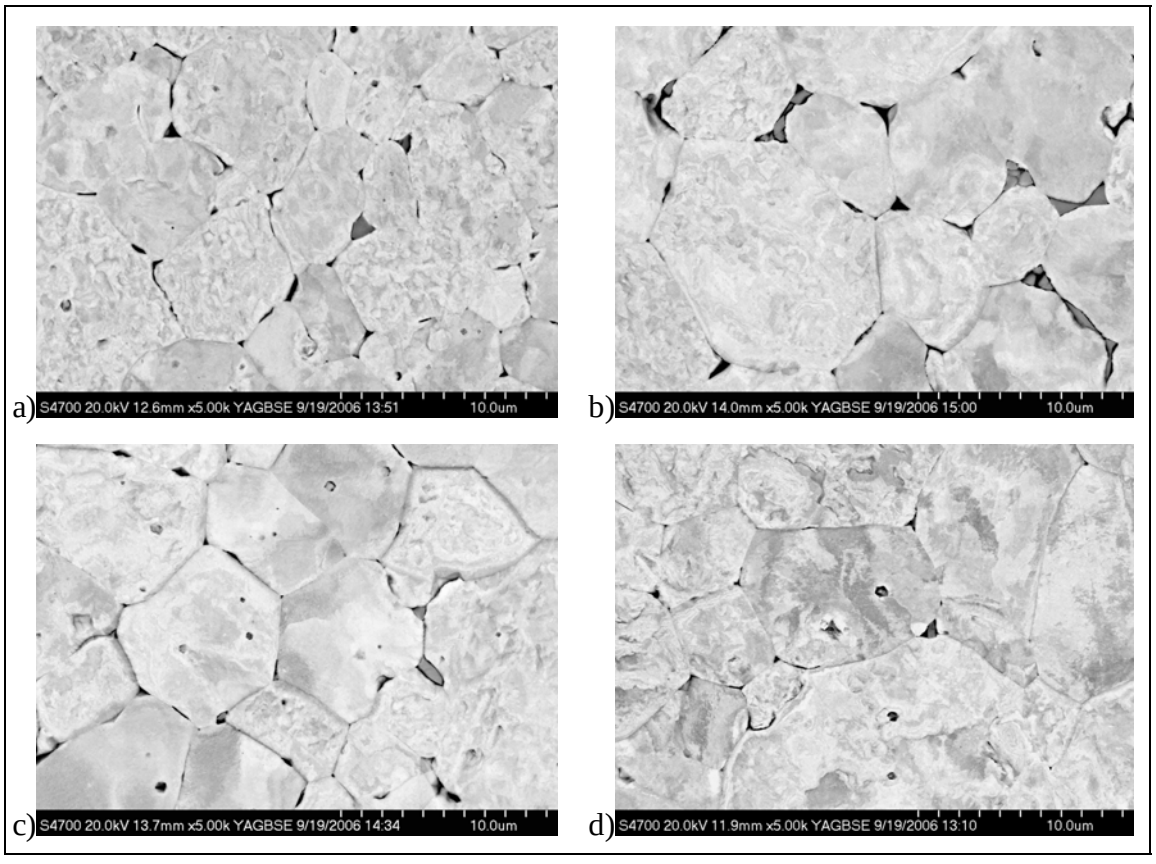

Figure 14. FESEM micrographs of P^2C consolidated M-10 tungsten with (a) no pretreatment, (b) hydrogen reduction, (c) pulsing, and (d) hydrogen reduction and pulsing.

The consolidated M-10 tungsten samples can be compared with those produced using the CNU nanopowders. The sample of M-10 powder with the highest sintered density (96.9% theoretical) had a grain size on the order of 5–10 μm. Processing of the CNU powders at lower temperatures resulted in samples with a grain size on the order of 500 nm. However, this retention of grain size came at the expense of sample density, as the highest density achieved for the CNU powder consolidated at 1200 ºC was 80.7% theoretical. Another previous study on P^2C consolidation of tungsten showed that for a submicron tungsten powder with average particle size between 0.7 and 0.99 μm, initial grain size was retained using a lower consolidation temperature, but final density was only 66.3% theoretical (*6*). A sintered microstructure from this sample is shown in figure 15. A comparison with the present study shows that an advantage of using nanopowders is the ability to achieve higher densities at the lower processing temperatures required to retain initial grain size.

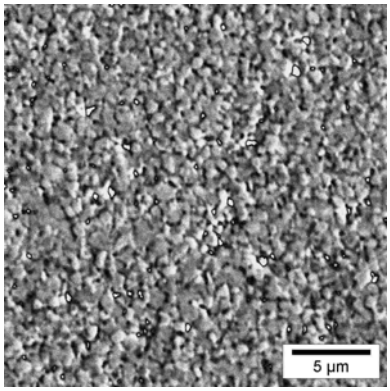

Figure 15. SEM micrograph of consolidated submicron tungsten powder showing retained initial grain size.

4. Conclusions

The purpose of this report was to characterize and evaluate the consolidation behavior of nanocrystalline tungsten powders produced at the Chungnam National University in Daejon, South Korea. The powders were shown to consist of nano-sized particles clustered into larger agglomerates. The powders also were found to contain higher levels of oxygen than conventional fine tungsten powder. The oxygen content was able to be reduced by a heat treatment procedure performed after powder production. It was possible to produce bulk samples with nano-sized grains by the P^2C method, but high density samples were not achieved. However, when compared with samples consolidated using conventional submicron tungsten powder, use of the CNU nanopowders was able to produce samples with higher densities at the lower temperatures required to retain initial grain size.

5. References

1. Magness, L. S.; Farrand, T. G. Deformation Behavior and its Relationship to the Penetration Performance of High Density Kinetic Energy Penetrator Materials, Durham, NC, *Proceedings of the 17th Army Science Conference*, Durham, NC, 1990, pp 149–165.

2. Cai, W. D.; Li, Y.; Dowding, R. J.; Mohamed, F. A.; Lavernia, E. J. A Review of Tungsten-Based Alloys as Kinetic Energy Penetrator Materials. *Reviews in Particulate Materials* **1995**, *3*, 71–132.

3. Wei, Q.; Jia, D.; Ramesh, K. T.; Ma, E. Evolution and Microstructure of Shear Bands in Nanostructured Fe. *Applied Physics Letters* **2002**, *81* (7), 1240–1242.

4. Wei, Q.; Jiao, T.; Ramesh, K. T.; Ma, E.; Kecskes, L. J.; Magness, L.; Dowding, R.; Kazykhanov, V. U.; Valiev, R. Z. Mechanical Behavior and Dynamic Failure of High-Strength Ultrafine Grained Tungsten Under Uniaxial Compression. *Acta Materialia* **2006**, *54* (1), 77–87.

5. Wei, Q.; Zhang, H. T.; Schuster, B.; Ramesh, K. T.; Ma, E.; Valiev, R. Z.; Kecskes, L. J.; Cho, K. C.; Dowding, R. J.; Magness, L. Microstructure and Mechanical Properties of Super-Strong Nanocrystalline Tungsten by High-Pressure Torsion. *Acta Materialia* **2006**, *54* (15), 4079–4089.

6. Cho, K.; Woodman, R.; Klotz, B.; Dowding, R. Plasma Pressure Compaction of Tungsten Powders. *Materials and Manufacturing Processes* **2004**, *19* (4), 619–630.

7. Cho, K.; Kellogg, F.; Klotz, B.; Dowding, R. Plasma Pressure Compaction (P^2C) of Submicron Size Tungsten Powder. *Proceedings of the International Conference on Tungsten, Refractory, and Hardmetals VI*, 2006.

8. McWilliams, B.; Zavaliangos, A.; Cho, K. C.; Dowding, R. J. The Modeling of Electric-Current-Assisted Sintering to Produce Bulk Nanocrystalline Tungsten. *JOM: Journal of the Minerals, Materials, and Metals Society* **2006**, *58* (4), 67–71.

9. Klotz, B. R.; Kellogg, F. R.; Klier, E. M.; Dowding, R. J.; Cho, K. C. *Characterization, Processing, and Consolidation of Nanoscale Tungsten Powder*; ARL-TR-5045; U.S. Army Research Laboratory: Aberdeen Proving Ground, MD, 2009.

NO. OF
COPIES ORGANIZATION

1 (PDF only) DEFENSE TECHNICAL INFORMATION CTR
DTIC OCA
8725 JOHN J KINGMAN RD
STE 0944
FORT BELVOIR VA 22060-6218

1 DIRECTOR
US ARMY RESEARCH LAB
IMNE ALC HRR
2800 POWDER MILL RD
ADELPHI MD 20783-1197

1 DIRECTOR
US ARMY RESEARCH LAB
RDRL CIM L
2800 POWDER MILL RD
ADELPHI MD 20783-1197

1 DIRECTOR
US ARMY RESEARCH LAB
RDRL CIM P
2800 POWDER MILL RD
ADELPHI MD 20783-1197

1 DIRECTOR
US ARMY RESEARCH LAB
RDRL D
2800 POWDER MILL RD
ADELPHI MD 20783-1197

ABERDEEN PROVING GROUND

1 DIR USARL
RDRL CIM G (BLDG 4600)

NO. OF COPIES ORGANIZATION

1 COMMANDER
US ARMY RDECOM ARDEC
AMSRD AAR AEE P
D KAPOOR
BLDG 60
PICATINNY ARSENAL NJ 07806-5000

1 COMMANDER
US ARMY RDECOM ARDEC
AMSRD AAR EM
J HEDDERICH
BLDG 94
PICATINNY ARSENAL NJ 07806-5000

1 COMMANDER
US ARMY REDECOM ARDEC
AMSRD AAR AEM J
G FLEMING
BLDG 65N
PICATINNY ARSENAL NJ 07806-5000

3 COMMANDER
US ARMY TACOM ARDEC
SFAE AMO MAS LC
R DARCY
R JOINSON
D RIGOGLIOSO
BLDG 354
PICATINNY ARSENAL NJ 07806-5000

1 US ARMY TARDEC
AMSRD TAR R
D TEMPLETON
6501 E 11 MILE RD
WARREN MI 48397-5000

1 US ARMY RDECOM
RDMR AEF T
J CHANG
BLDG 4488 RM B274
REDSTONE ARSENAL AL 35898

2 US ARMY RDECOM
RDMR AEF
G LIU
R MCFARLAND
BLDG 4488
REDSTONE ARSENAL AL 35898

NO. OF COPIES ORGANIZATION

3 US ARMY RSRCH OFFICE
J PRATER
D STEPP
D KISEROW
PO BOX 12211
RSRCH TRIANGLE PARK NC
27709-2211

ABERDEEN PROVING GROUND

26 DIR USARL
RDRL WM
J SMITH
S KARNA
J MCCAULEY
P PLOSTINS
RDRL WML
M ZOLTOSKI
J NEWILL
RDRL WML H
L MAGNESS
B SCHUSTER
RDRL WMM
R DOWDING
J ZABINSKI
RDRL WMM A
M MAHER
RDRL WMM B
M VANLANDINGHAM
RDRL WMM D
E CHIN
K CHO
RDRL WMM E
M PEPI
RDRL WMM F
B BUTLER
W DE ROSSET
L KECSKES
F KELLOGG
E KLIER
B KLOTZ
H MAUPIN
RDRL WMM G
A RAWLETT
RDRL WMP
P BAKER
S SCHOENFELD

INTENTIONALLY LEFT BLANK.